Nonlinear refraction and multiphoton absorption in polydiacetylenes from 1200 to 2200 nm

Sergey Polyakov,* Fumiyo Yoshino,† Mingguo Liu,‡ and George Stegeman
School of Optics and Center for Research and Education in Optics and Lasers, University of Central Florida, 4000 Central Florida Boulevard, Orlando, Florida 32816-2700, USA

(Received 21 July 2003; revised manuscript received 5 November 2003; published 22 March 2004)

We report femtosecond measurements of the dispersion in the nonlinear refraction and multiphoton absorption in polydiacetylenes, specifically in PTS [polymer poly (bis para-toluene sulfonate) of 2,4-hexadiyne −1,6 diol] over the spectral range 1200 to 2200 nm. Various modifications of the *Z*-scan technique were used to make the measurements. The nonlinear refractive index coefficient n_2 decreased monotonically with wavelength and can be reasonably extrapolated to previous measurements at 1064 nm. It was found that multiple multiphoton absorption mechanisms contributed to the nonlinear absorption at most wavelengths so that the intensity dependence at each wavelength was needed to identify the different contributions. A two-photon absorption coefficient decreasing monotonically with increasing wavelength was identified with the long wavelength tail of the massive two-photon absorption peak measured previously at 930 nm. The three-photon absorption coefficient showed a weak resonance around 1850 nm associated with the one-photon absorption into the odd symmetry peak at 620 nm, but also exhibited larger values at shorter wavelengths whose assignment is not clear. The four-photon coefficient, measurable only around 1900 nm was associated with four-photon absorption into the even symmetry 465 nm state responsible for strong two-photon absorption measured previously at 930 nm. This resonance, normally much too weak to be observed, was measurable only because of the accidental degeneracy with the three-photon absorption resonance. This degeneracy also leads to a single photon excited state absorption into the 465 nm state via an initial three-photon absorption into the odd symmetry 620 nm state. It was shown that this $(3+1)$ process is in the saturation regime over the intensity range of the measurements and does not contribute to absorption change proportional to the cube of the input intensity, which indicates the pure four-photon absorption process. Thus the measured four-photon coefficient was identified to be due to true instantaneous four-photon absorption. Finally, polarization-dependent *Z*-scan was used to evaluate the difference between the linear and nonlinear absorption coefficients parallel and perpendicular to the polymer's conjugation axis and to crosscheck the nonlinear measurements made via *Z*-scan. The differential linear absorption coefficient was found to be in a good agreement with that measured by a standard spectrophotometer measurement.

DOI: 10.1103/PhysRevB.69.115421 PACS number(s): 42.70.Mp, 42.70.Nq, 42.65.−k, 82.35.Ej

I. INTRODUCTION

Polydiacetylenes are essentially one-dimensional (1D) quantum wires in terms of their optical properties.[1–3] They consist of a quasilinear chain of carbon atoms bonded by single, double, and triple bonds. The key point is that a carbon atom has four valence electrons that occupy the $2s$, $2p_x$, $2p_y$, and $2p_z$ orbitals. Upon the formation of the conjugated polymer chain the *s* and *p* orbitals overlap to form σ and π bonds, respectively. In the case of alternating double (or triple) bonds, the single atom $2p_z$ (and $2p_y$) orbitals that lie orthogonal to the σ bond, form a continuous orbital in which electrons can move more or less freely parallel to the carbon-carbon axis, the polymer ''backbone.'' The facile movement of the π electrons results in the large polarizabilities (and hyperpolarizabilities) observed in conjugated polymers. Although the polymer backbones are usually separated by side groups bonded approximately orthogonal to the polymer axes, these groups contribute electronic states in the deep blue and UV whereas the conjugation leads to electronic states in the visible and near infrared. Thus the electronic states associated with the polymer's backbone reflect the linear symmetry of the polymer backbone and have either even (A_g) or odd (B_u) symmetry.[4,5] The ground state is $1A_g$ (labeled 0) and the first one-photon active excited state (exciton) is $1B_u$ (labeled 1).

The special properties of conjugated polymers were recognized in the late 1960's and early 1970's by Wegner and colleagues.[1] Many interesting properties were investigated over the succeeding years, including the excitonic nature of the dominant and very intense absorption peak in the optical absorption spectrum, the excitation of triplet states and the photoactivated conductivity.[6–8] However, it was Sauteret and co-workers that stimulated the interest in these materials as nonlinear optical materials. Using third harmonic generation (THG) they estimated the nonresonant, intensity dependent refractive index coefficient n_2 to be 2×10^{-12} cm^2/W in single crystals of the polydiacetylene PTS [polymer poly (bis para-toluene sulfonate) of 2,4-hexadiyne-1,6 diol].[9] Here the optically induced refractive index change Δn is given in terms of the local intensity by $n_2 I$ where $n_2 \propto \mathrm{Re}[\chi^{(3)}(-\omega;\omega,-\omega,\omega)]$ and $\chi^{(3)}$ is the third order susceptibility. Soon thereafter Lequime and Hermann reported large two-photon absorption coefficients $\alpha_2 \propto \mathrm{Im}[\chi^{(3)}(-\omega;\omega,-\omega,\omega)]$.[10] These two papers pioneered nonlinear optics in polydiacetylenes in general, and single crystal PTS in particular.

In the succeeding years there were numerous measurements in PTS and associated polydiacetylenes of the third order susceptibility in general, and of the nonlinear refractive index. Most of these measurements were done near wave-

lengths at which the dominant electric dipole $1A_g \rightarrow 1B_u$ transition dominates the nonlinear response. The wavelength dispersion of third harmonic generation was used to identify the location of two-photon absorbing states.[11] Degenerate and nondegenerate four wave mixing, and spectral broadening due to self-phase modulation were used to evaluate $|\chi^{(3)}(-\omega;\omega,-\omega,\omega)|$.[12–18] *Z*-scan and interferometry was used to measure both n_2 and α_2, primarily at 1064 nm.[17,19–24]

The values reported for the nonlinear coefficients of polydiacetylenes can vary by factors of 2 or more, and even disagree in the sign of the nonlinearity. We believe that there are a number of reasons for this. First amorphous polymers can have different degrees of conjugation, depending on the preparation conditions.[25,26] Secondly, even in crystals the sample morphology can depend on the crystallization and polymerization conditions. Thirdly, when single crystal polymers are formed from single crystal monomers, there is significant bond rearrangement that occurs which leads to strains and defects in the crystals.[27] The values of the nonlinearities on the crystals prepared here are consistent with those measured on crystals supplied by two other research labs.[7,11]

Nonlinear measurements are driven by potential applications to all-optical signal processing.[28] They rely on a large n_2 in spectral regions where the linear and nonlinear absorption is minimal at the intensities required for device operation. Polydiacetylenes, both amorphous and single crystal, have been used for such devices with mixed success in the near infrared.[29–32] No devices have been reported yet in the communications bands. Here we report the full dispersion of the nonlinear index coefficient n_2 from 1200 to 2200 nm.

The present work is also driven by the large one- and two-photon absorption already reported in the near infrared.[10,23,24] They raise the possibility that even higher order multiphoton absorption should occur in the 1200–2200 nm spectral band. Although resonantly enhanced three-photon absorption ($\Delta\alpha = \alpha_3 I^2$) has been demonstrated previously in organic materials, under normal circumstances four-photon absorption is much too weak to be observed.[33] For example, there have only been sporadic, and in some cases disputed, reports of four-photon absorption ($\Delta\alpha = \alpha_4 I^3$) in semiconductors,[34] but none to date, to the best of our knowledge, in molecular solids except for the weak four-photon absorption reported previously in this spectral region in PTS.[35] In principle this effect can be observable if there is an additional resonant enhancement mechanism in play, and in fact we show here that this is the case. It turns out there is more than one contributing multiphoton mechanism at every wavelength in this spectral range which necessitated the intensity dependence analysis of multiphoton absorption at each wavelength investigated. Here we report the spectral variation in two-, three-, and four-photon absorption in the wavelength range investigated.

This paper is organized as follows. In Sec. II we discuss the electronic states previously measured in PTS and how they affect multiphoton absorption. A summary of the fabrication procedures used in making the PTS single crystals is given in Sec. III. The measurement techniques and the data reduction, including the difference in the linear absorption between orthogonal polarizations are discussed in Sec. IV. Also, Sec. IV includes a brief discussion of the impact of self-focusing on the reliability of the measurements, which sets the limit on a maximum sample length and maximum intensities that can reliably be used for the nonlinear characterization. Section V summarizes the measurements on the dispersion of nonlinear refractive index and the two-, three-, and four-photon absorption. Contributions to an effective four-photon process from three-photon absorption followed by excited state absorption are discussed in Sec. VI. We summarize the work in Sec. VII.

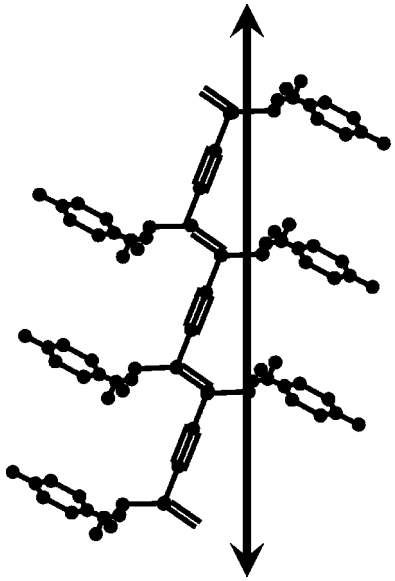

FIG. 1. Chemical structure of PTS.

II. ELECTRONIC STATES IN POLYDIACETYLENE PTS

The molecular structure of single crystal PTS is very well known and is shown in Fig. 1.[1–3] In the first approximation the electronic excited states associated with the spacer units that occur in the near ultraviolet and deep blue regions of the absorption spectrum are decoupled from those associated with the single, double and triple C-C bonds where π electrons are delocalized along the polymer chain and occur in the visible. As a result, in the visible the electronic states reflect quasilinear symmetry and the states are either even A_g or odd B_u symmetry. Since one-photon electric dipole active transitions between energy levels involve a change in state parity, they occur between the A_g and B_u states. Similarly for two-photon electric dipole transitions, the initial and final states both have the same parity, but are mediated by a state with the opposite parity. In general, transitions involving an odd number of photons require initial and final states of different parity and for an even number of photons the initial and final states exhibit the same parity.

One-photon absorption (1PA) and two-photon absorption (2PA) spectroscopy have identified the even (mA_g) and odd ($1B_u$) symmetry states with the largest electric dipole transition moments linked to electron excitation from the even symmetry ground state $1A_g$. Shown in Figs. 2(a) and 2(b)

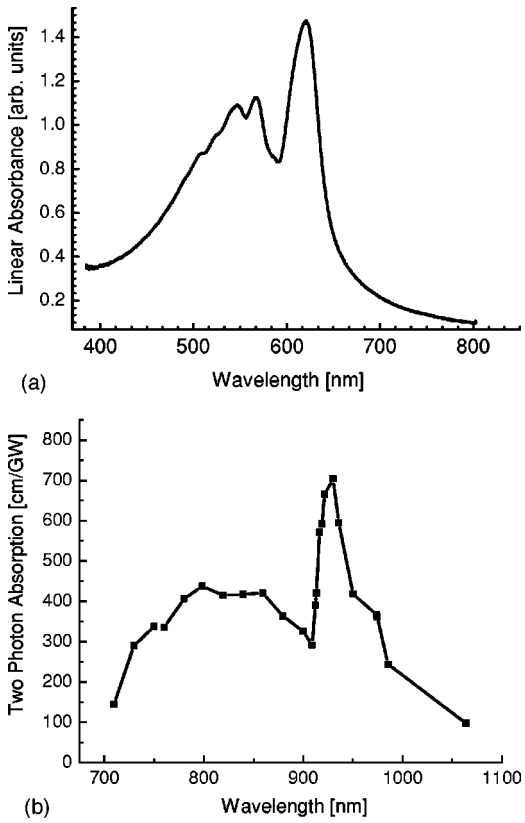

FIG. 2. (a) One-photon absorption spectrum taken with the incoming polarization parallel to the polymerization bone and (b), two-photon absorption spectrum from Ref. 24 taken with polarization parallel to the polymerization bone.

are the measured spectra.[23,24,36] The one- and two-photon peaks occur at 620 and 930 nm, respectively, and identify the $1B_u$ and mA_g (labeled 2) states as lying 2.0 and 2.7 eV above the ground state. Note that the ratio between these energy levels $E_{mAg}/E_{1Bu}=4/3$. The approximate location and oscillator strengths are in good agreement with theory.[37–40] Although the progression of excited states in terms of energy above the ground state, for example for electrons in a 1D box, is usually $1B_u$, $2A_g$, $2B_u$, $3A_g$, etc., strong electron correlation effects exist in polydiacetylenes and there is a weakly coupled, even symmetry state lying just below the $1B_u$ state which appears to play no role in our experiments.[4,11,37,38]

Both the one- and two-photon absorption spectra exhibit strong side bands towards the shorter wavelength side of the main peak. These have been identified as vibronic sidebands due to transitions within the vibrational manifolds of the electronic states.[4,6] As a result the total oscillator strength of these transitions is spread out in wavelength and the observed overall spectral width is not indicative of the excited state lifetimes. These have been measured by pump-probe spectroscopy to be about 2 ps for the $1B_u$ to $1A_g$ decay and about 100 fs for mA_g to $1B_u$.[15,41–44]

The peak values of the linear and two-photon absorption coefficients are $\alpha_1=7\times10^5$ cm^{-1} (at 620 nm) and $\alpha_2=7\times10^2$ cm/GW (at 930 nm), respectively. These values are so large that they raise the possibility of measuring the next

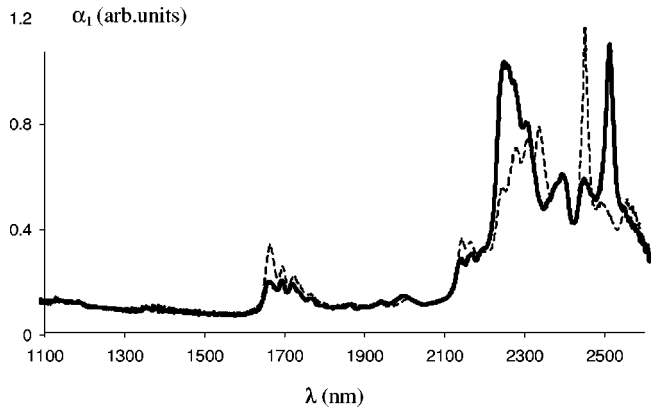

FIG. 3. Linear absorption spectrum of PTS in the transparency region (between the strong absorption peaks in the visible due to π electron levels and in the infrared due to strong vibronic resonances of the C bonds). The solid thick line light was obtained with light polarized parallel to the polymerization direction and the thin dashed line with light polarized perpendicular to the polymerization direction.

higher order nonlinear absorption, namely, three- and four-photon absorption. To estimate the multiphoton absorption values we used perturbation theory which incorporates knowledge of the strongest odd ($1A_g$ to $1B_u$) and even ($1A_g$ to mA_g) photon absorption resonances. This gives the following approximations for the resonant terms of $\chi^{(5)}(-\omega;\omega,-\omega,\omega,-\omega,\omega)$ and $\chi^{(7)}(-\omega;\omega,-\omega,\omega,-\omega,\omega,-\omega,\omega)$, which are the origin of three-photon absorption (3PA) and four-photon absorption (4PA), respectively:[45]

$$\alpha_3 \propto \frac{|\mu_{01}|^6}{(\omega_{01}-3\omega-i\Gamma_{01})} f(\omega,\omega_{01},\ldots),$$

$$\alpha_4 \propto \frac{|\mu_{01}|^6|\mu_{12}|^2}{(\omega_{01}-3\omega-i\Gamma_{01})^2(\omega_{02}-4\omega-i\Gamma_{02})} \times F(D,\omega,\omega_{01},\omega_{02},\ldots).$$

Here μ_{01} and μ_{12} are the electric dipole transition moments from $1A_g$ to $1B_u$ and $1B_u$ to mA_g, respectively. This approximate model is essentially useful for finding the ratio between the three-and four-photon absorption coefficients and for giving rough order of magnitude estimations for these coefficients. For estimating the order of magnitude of α_3 and α_4, the dipole transition moments above could be assumed equal. The one- and two-photon transition energies are $\hbar\omega_{01}$ and $\hbar\omega_{02}$, respectively, and Γ_{01} and Γ_{02} are the linewidths associated with the upper state lifetimes. Finally, the functions $f(\omega,\omega_{01})$ and $F(D,\omega,\omega_{01},\omega_{02})$ are expected to be slowly varying functions of frequency with $D=|\mu_{12}/\mu_{01}|$. The exact form of these functions depends on the contribution of vibrational degrees of freedom and resonances due to lattice defects which are one-photon active. The photon energies associated with 3PA and 4PA fall into the absorption bands associated with vibrational overtones. Shown in Fig. 3 is the absorption spectrum measured in that spectral region.

In PTS the transition dipole moments from the ground state to $1B_u$ and from the $1B_u$ to mA_g states are reported to be very large—over 3 eÅ.[40,46] In addition to this, in PTS $E_{mAg}/E_{1Bu}=\frac{4}{3}$ so that there is an accidental degeneracy between three-photon ($3\times620=1860$ nm) and four-photon ($2\times930=1860$ nm) absorption. Keeping just the leading resonant terms for this case $\mathrm{Im}(\chi^{(7)})_{\mathrm{3PA\ enhanced}} \approx \mathrm{Im}(\chi^{(7)})_{\mathrm{nonenhanced}}[\omega_{01}^2/\Gamma_1^2]$. This degeneracy provides an enhancement mechanism which might make four-photon absorption 4–5 orders of magnitude larger, and this factor would depend on the relative position of the resonances. It is a straightforward exercise to show that with no accidental degeneracy, four-photon absorption detection would require peak intensities which easily damage the crystal.

III. SAMPLE PREPARATION

Since Wegner's pioneering work, topochemically controlled solid state polymerization of monomer diacetylene crystals has been used successfully to prepare large polymer single crystals.[1–3,36] The best known compound of this family is the symmetric diacetylene referred to as pTS or PTS (pTS as monomer and PTS as polymer). Centimeter size monomer pTS crystals can be grown by a slow solvent evaporation technique from saturated acetone solution.[47,48] The polymerization of monomer pTS molecules can be easily initiated by thermal annealing or by exposure to radiation (x ray, γ ray), even at room temperature and in ambient light. This solid state reaction results in a long conjugated chain along the crystallographic *b* axis, essentially leading to polymer PTS crystal growth within the ''template'' of the monomer pTS crystal structure. This approach with some important modifications was used in our crystal preparation.[36]

The pTS material was synthesized by the well known procedures.[1–3,9] Successive recrystallization from acetone was used to purify the pTS. After the purification, the pTS acetone solution became nearly colorless.

The polymerization process, both during growth of the monomer and the subsequent monomer to polymer conversion was found to be critical to producing samples with a minimum of defects.[36] pTS crystallizes in the monoclinic space group $P2_1/c$ with $a=1.460$ nm, $b=0.515$ nm, $c=1.502$ nm, and $\beta=118.4°$. After polymerization, the space group remains the same while the cell parameters change to $a=1.448$ nm, $b=0.493$ nm, $c=1.491$ nm, and $\beta=118.0°$.[49] The drastic shrinkage of 5% along the *b* axis is typically the cause of defects, etc. Two steps were taken to control the polymerization. The growth procedure used minimized the polymerization to maintain a stable surface cell structure at the growth interface, thus achieving a smooth development of pTS facets. Second, the annealing process during polymerization was carefully designed.

Monomer crystals were grown by self-nucleation in a vessel housed in a sealed glass jar with controlled nitrogen flow passing through it. The growth process was performed relatively quickly to inhibit polymerization, in about 60 h after the nucleation. Each monomer crystal had well-developed crystallographic facets and dimensions greater than 1 cm. The large facet (001) exhibited a perfect cleavage plane, facilitating cleaving into thin pieces prior to polymerization. The monomer crystals were very light pink after growth, implying very low polymer conversion during the short growth period. However, the color quickly changed to red when left at room temperature indicating that polymerization had subsequently occurred.

A typical polymerization conversion curve exhibits a characteristic S shape. It consists of an induction period to about 10% conversion followed by a rapid rise up to 90%, and then a gradual increase to the completion of the conversion. It is in the rapid rise region that the drastic change in the cell parameter occurs, probably accompanied by catastrophic cracking inside the crystals. The PTS conversion curves at different temperatures show similar *S*-type characteristics, but were progressively steeper in the rapid rise region with increasing temperature.[49,50] Thus decreasing the annealing temperature (from 60 to 45 °C) slowed down the 10–90 % conversion process, and made the cell parameter change more slowly in this critical period. A reduction in crack defects was observed with this scheme. Typically, nearly perfect polymer crystals less than 1 mm thick could be obtained after polymerization, whereas samples several mm thick did show evidence of cracks.

The net result was samples superior to those on which the original measurements of multiphoton absorption and refraction were performed.[21–23,35] More details can be found in Ref. 36.

IV. MEASUREMENT AND ANALYSIS TECHNIQUES

The measurement technique chosen is *Z*-scan, schematic shown in Fig. 4(a). In this technique a sample is moved through the focus of a beam and the transmitted signal is either completely (open aperture for multiphoton absorption) detected, or just sampled over a small aperture centered on the beam axis (closed aperture for evaluating n_2).[51] As the sample is moved, the diameter of the beam changes and hence the sample cross-sectional area studied changes. In samples such as PTS where scattering due to defects occurs in the bulk regions, additional spurious changes in the transmission can appear as the sample is moved.

In order to avoid this problem, alternative versions of *Z*-scans were introduced. ''Power scan'' was chosen for closed aperture measurements and ''polarization scan'' was used in an open aperture geometry as an ultimate proof that the signal observed is due to a nonlinear versus a spurious position-dependent response [Figs. 4(b) and 4(c)]. In these techniques the sample remains fixed in position near the focus, and the power or polarization of the incoming light is changed. To measure a nonlinear refractive index change with power scan, the sample is placed at the peak of the standard closed aperture *Z*-scan curve to monitor the change in ΔT_{p-v} whereas to measure the intensity dependent absorption with polarization scan, the sample was located exactly at the focal point of the beam which maximizes the nonlinear absorptive response. While for power scan the overall peak intensity of the incoming light is changed, the polarization-scan method takes advantage of the strong polarization anisotropy (1D) of

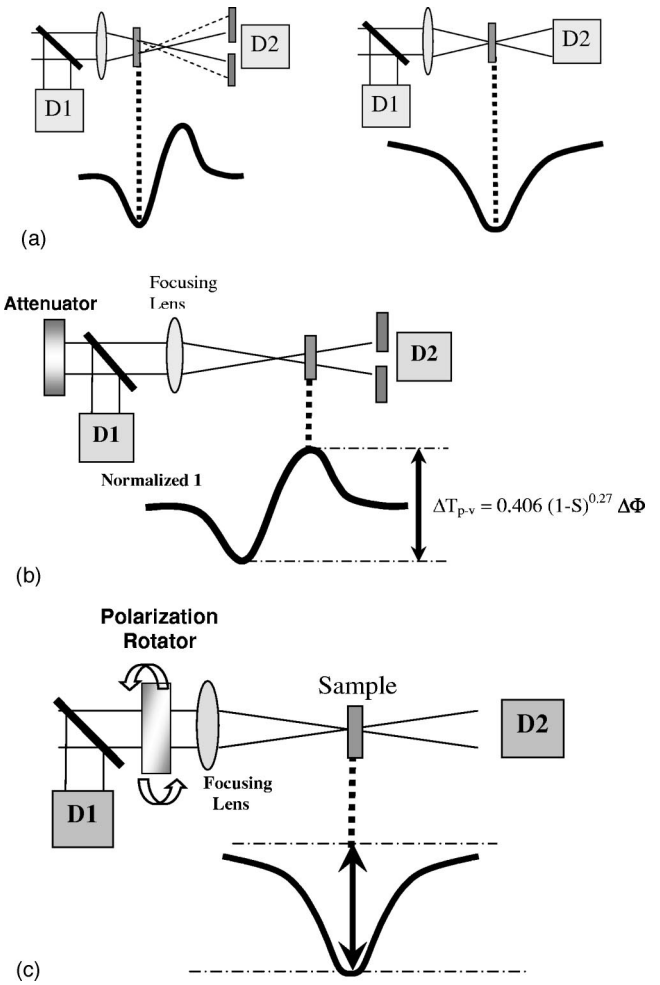

FIG. 4. Experimental realization of a *Z*-scan (a) and its variations: power scan (b) in which the input intensity is changed ($\Delta\Phi$-maximum phase shift; *S*-aperture transmission) and polarization scan (c) in which the polarization of the incident beam is varied.

the nonlinear response of polydiacetylenes. The polarization is varied by a wavelength-independent liquid crystal-based polarization rotator. Furthermore, when the sample is placed in a large diameter part of the beam, the difference in the transmission between the two orthogonal polarizations yields the differential linear absorption coefficient between those polarizations.

It has previously been shown that the combination of the large $\Delta n(I)$ and $\Delta\alpha(I)$ found in PTS can lead to sufficient beam distortion at high intensities that *Z*-scan can lead to misleading results.[52] This occurs in two limits. If the multiphoton absorption is strong, the beam becomes flattened on propagation and the edges of the flat region develop diffraction rings which can be amplified by strong self-focusing. Alternatively, self-focusing can occur which narrows the beam and increases dramatically the peak intensity so that multiphoton absorption becomes dominant. Neither of these effects is contained in the standard *Z*-scan analysis techniques. They could have been the origin of the distortions in *Z*-scan data at high intensities which led to interpretations in terms of n_3 and α_3.[22] These problems can be avoided in PTS by operating with short enough samples so that these complications, which require sufficient propagation distance to occur, are absent. This criteria limits sample thicknesses to about 200 μm in this case.[52]

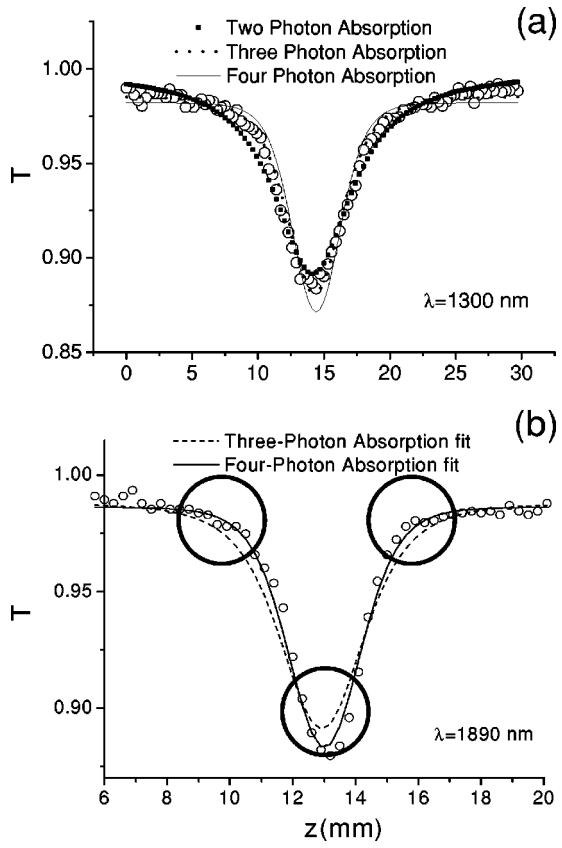

FIG. 5. Examples of *Z*-scan measurements (circles) at two different wavelengths (a) 1300 nm (dominated by three-photon absorption) and (b) 1890 nm (dominated by four-photon absorption).

The light source was a spectra-physics/positive light optical parametric generator/amplifier (OPG/OPA). It produces 100 fs pulses at a 1 kHz repetition rate with individual pulses of energy up to 20 μJ with spectral bandwidths of 40 nm over the wavelength range 1200 to 2200 nm, which produce peak intensities up to 50 GW/cm^2 incident on the sample at focus. Custom made thermoelectrically cooled InAs detectors by EG&G with sensitivity out to 2200 nm were used.

The open aperture *Z*-scan by itself is not very sensitive to the order of the multiphoton absorption. Examples at two wavelengths are shown in Fig. 5. Shown in Fig. 6(a) is the intensity dependence of the fit to each order of absorption made by setting all of the other nonlinear coefficients to zero. If only one order of the nonlinear absorption was involved analyzing the data as either just 2PA, or just 3PA, or just 4PA would result in a constant multiphoton absorption coefficient which is independent of intensity. To the contrary, the curves seen in Fig. 6(a) strongly vary with intensity, and therefore, the assumption that the multiphoton process of only one kind, 2PA or 3PA or 4PA, was present fails.

As just discussed previously, scanning the input polarization with a fixed sample position was also implemented. Typical results are shown in Fig. 7. The period of oscillations observed in Fig. 7 clearly indicates the one-dimensional na-

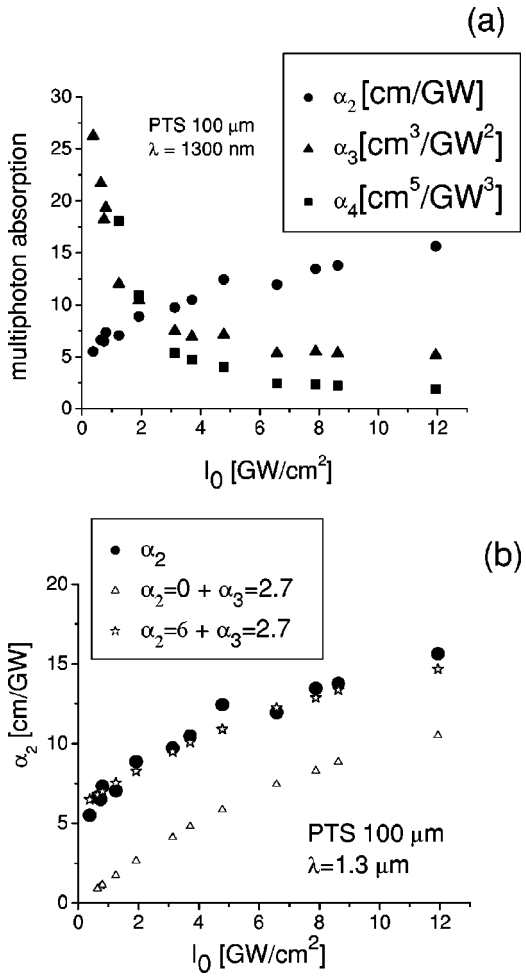

FIG. 6. Data interpretation with mixed orders of multiphoton absorption allows an extraction of two independent multiphoton absorption coefficients. (a) Experimental data fits to the model that only 2PA (circles), only 3PA (triangles), or only 4PA (squares) is present. Two-, three-, and four-photon absorption are given in the units of cm/GW, cm^3/GW^2, and cm^5/GW^3, respectively. (b) The same dataset fit to the model with only 2PA is present (circles) exhibits similar intensity dependence as the simulated 3PA (2.7 cm^3/GW^2) fitted to the 2PA model (triangles); the offset between the two graphs (circles and triangles) is almost constant, 6 cm/GW. Finally we assume both 2PA (6 cm/GW) and 3PA (2.7 cm^3/GW^2) present and simulate new *Z*-scans. The 2PA fit obtained from the experiment (circles) is then compared with the final 2PA fit to the simulated *Z*-scan (stars).

ture of the nonlinear response. Furthermore, the differences between the fits of the various multiphoton processes, one at a time, does not lead to large differences in the shape of the response, indicating again that fitting to the raw data alone is not conclusive for determining the order of the nonlinear absorption.

Various approaches were used in attempts to identify and quantify the various processes involved. Analyses based on the raw *Z*-scan data were attempted first. For example, the intensity dependence shown in Fig. 5(b) indicates that 4PA may be the dominant process at that wavelength. However, least squares fitting of such data to 3PA [giving α_3 (effective)] or 4PA [giving α_4 (effective)] did not lead to large enough differences in χ^2 for indisputable assignment. Also, by just performing least squares fitting to the regions in which the differences between the theoretical curves in Fig. 5(b) were the largest, circled in Fig. 5(b), also did not lead to useful results. It was finally concluded that the contributions from the different processes could not be separated from the raw *Z*-scan data.

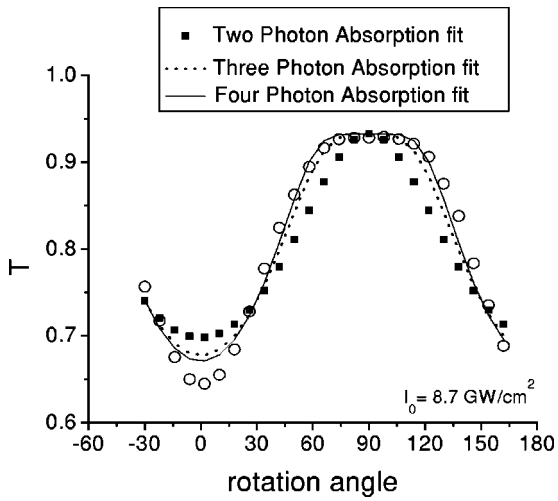

FIG. 7. Polarization scan traces (circles) at the wavelength 1300 nm and the best fits to each of the three multiphoton absorption coefficients.

However, the intensity dependence in plots such as those shown in Fig. 6 does contain information about all of the orders present. This intensity dependence in fact confirms the presence of other absorption process. Since the intensity dependence originates from a missing order of absorption, it can be compared to the intensity dependence of a curve which was produced by fitting simulated (calculated) *Z*-scan curves with the missing multiphoton absorption order included, i.e., ''synthetic *Z*-scans'' [open triangles in Fig. 6(b)]. In this way the magnitude of the other order process can be estimated. The linear difference between the experimental data fit and the fit from the synthetic *Z*-scans with the missing order included gives approximately the value of the multiphoton absorption fitted (2PA in this example). As the next step, a new set of synthetic *Z*-scans were generated using both of the two estimated coefficients (α_2 and α_3). The two coefficients were then adjusted until the intensity dependence of the fitted plot agrees with the one obtained from the experimental data fit. The same process was repeated for fitting to the α_3 (effective) or α_4 (effective). Note that the curves deduced from the experimental data can be reproduced quite accurately [star in Fig. 6(b)] by a single choice of a pair of multiphoton coefficients for all intensities studied. The resulting error bars on the fits are shown later when the final results are discussed. The same overall philosophy of analyzing data at a given wavelength as a function of intensity was employed for deducing the nonlinear refraction coefficient. In contrast to the previous discussion, however, all of the cases analyzed led to an intensity independent n_2 at each wavelength. Thus only a single nonlinear refraction process giving $\Delta n = n_2 I$ was measurable.

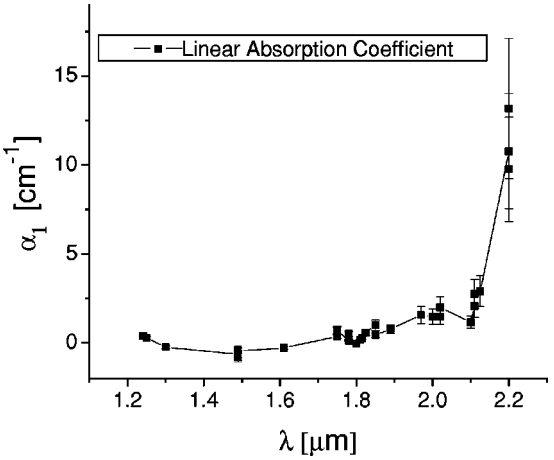

FIG. 8. Wavelength dependence of the linear absorption measured in the polarization scan technique at low input intensities. The solid line is a guide to the eye and not a fit to the data.

The difference in linear absorption between the two polarizations was taken into account as a function of wavelength using polarization scan at low input intensities. The results shown in Fig. 8 are consistent with the standard spectrometer results, Fig. 3.

V. NONLINEAR COEFFICIENTS

The nonlinear coefficients n_2, α_2, α_3, and α_4 measured are shown in Figs. 9–13. The nonlinear refraction coefficient is shown in Fig. 9 and the fitted values of the two-photon (α_2), three-photon (α_3), and four-photon (α_4) absorption coefficients are shown in Figs. 10–13.

The coefficient n_2 is positive and decreases monotonically with increasing wavelength over the range investigated. It can be reasonably extrapolated to the value $n_2 = 50(\pm 10) \times 10^{-4}$ cm^2/GW measured at 1064 nm on samples produced in another laboratory, completing the picture of the wavelength variation of n_2 from 620–2200 nm.[21,22] For 620 nm $< \lambda <$ 930 nm, $n_2 < 0$.[24,53,54] There is a change in sign in the vicinity of the large two-photon absorption peak at 930 nm

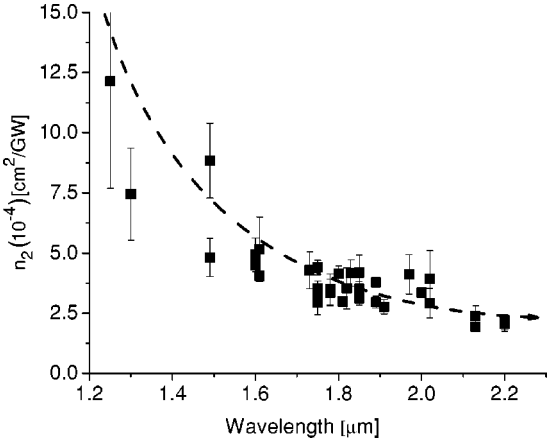

FIG. 9. Measured wavelength dispersion of the intensity dependent refractive index coefficient (squares) and its extrapolation (dashed line).

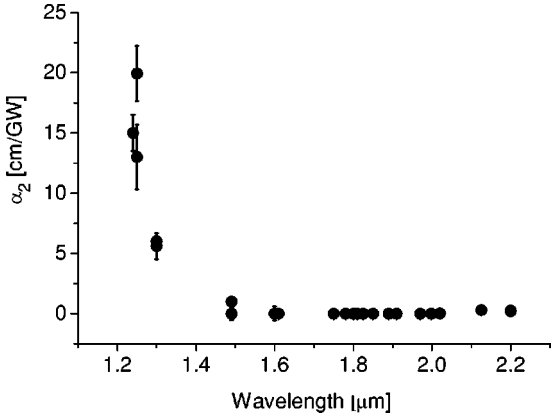

FIG. 10. Wavelength dispersion of the two-photon absorption coefficient.

and there-after n_2 decreases monotonically for increasing λ. Note that although $\lambda = 2200$ nm is far from the nearest electronic resonance (2PA at 930 nm), n_2 is still slowly decreasing with increasing wavelength. Finally, no evidence was found for any additional dispersion in nonlinear refraction in the vicinity of 1850 nm, indicating that the contribution to $\Delta n(I)$ from the next higher order coefficient n_3 is negligible for intensities up to few GW/cm^2.

Consider next the two-photon coefficient, Fig. 10. It decreases monotonically to zero (immeasurably small values) and extrapolates to the value $\alpha_2 = 100\ (\pm 25)$ cm/GW at $\lambda = 1064$ nm measured in samples from a different source.[21,22] In this spectral region, the monotonic decrease in α_2 with increasing wavelength is associated with the tail of the strong 2PA peak (>700 cm/GW) at 930 nm.[23,24] However, no evidence was found for the additional two-photon peaks reported previously at longer wavelengths using 25 ps pulses.[23] In that work all maxima due to multiphoton absorption were identified as having a two-photon origin and clearly that assignment was in error.[23]

The three-photon absorption response is shown in Figs. 11 and 12. For the shorter wavelengths investigated, α_2 domi-

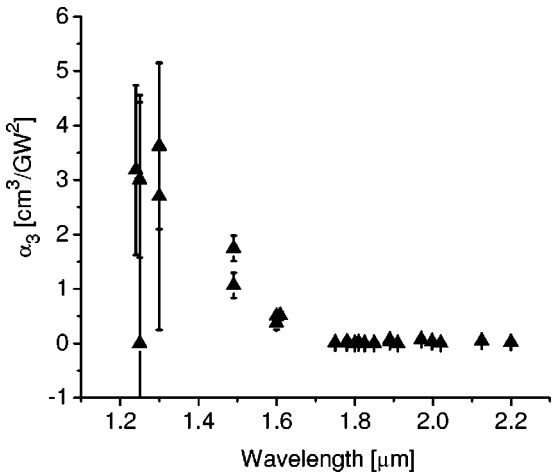

FIG. 11. Wavelength dispersion of the deduced three-photon absorption coefficient.

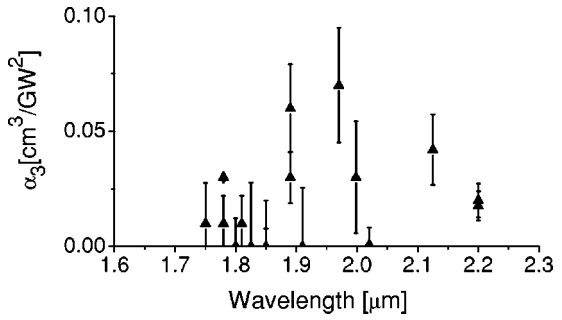

FIG. 12. Three-photon absorption near the wavelength of its expected resonance at about 1900 nm.

nated the nonlinear absorption so that the error bars for α_3 are large. At longer wavelength, around 1800–1900 nm, shown in blow-up format in Fig. 12, only a weak enhancement is observed. An order of magnitude estimate for the peak value of resonantly enhanced α_3 is 0.1 cm^3/GW^2.

Unexpected is the rise in α_3 starting at around 1600 nm and extending to the shortest wavelengths studied. Even discounting the data below 1400 nm due to the large error bars, there is definitely multiphoton absorption between 1400 and 1600 nm. This could be the peak previously identified as two-photon absorption with a maximum around 1400 nm.[23] Furthermore, the response between 1200 and 1300 nm may be associated with another peak also reported in that earlier work.[23] However, there is a clear difficulty in assigning a feature (around 500 nm) in the one-photon absorption to the better defined of these two peaks. We do note that there is a broad and weak shoulder to the linear absorption spectrum centered at 500 nm, see Fig. 2(a). Note also that electroabsorption spectroscopy has suggested that the onset of the ''continuum'' of states occurs at 2.4 eV (500 nm), a feature that is not believed to appear in the linear absorption spectrum, and this three-photon absorption could be associated with multiphoton absorption due to this effect.[55]

It is known that other physics in the polydiacetylenes gives a α_3-like response. For example, Kobayashi[56] has reported a process in the polydiacetylene 3BCMU which peaks at about 810 nm and decays monotonically towards 1100 nm. He refers to an interexciton interaction (Auger recombination followed by fission) as a probable cause for this $\chi^{(5)}$ effect.

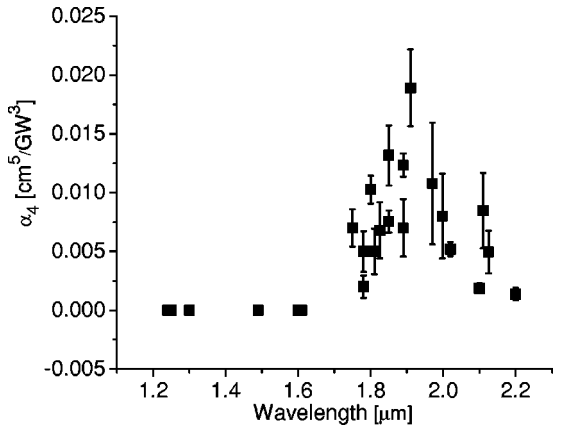

FIG. 13. Wavelength dispersion of the deduced four-photon absorption coefficient.

Finally, the four-photon absorption spectrum showed (Fig. 13) a distinct maximum in the region 1700 to 2200 nm, with a well-defined peak at 1900 nm. This corresponds closely with the peak position predicted by the much better defined two-photon spectrum, namely, 1860 nm. Note that if we compare the induced absorption coefficient at 20 GW/cm^2 at 1900 nm, the contribution to the absorption from α_3 is about 20 cm^{-1} whereas that from α_4 is 80 cm^{-1}, indicating that α_4 dominates the data at such high intensities.

VI. INTERPRETATION OF THE FOUR-PHOTON ABSORPTION SPECTRUM

There are two obvious physical pathways by which a four-photon response can be obtained in PTS. The previous discussion has centered on instantaneous 4PA, enhanced by an accidental degeneracy with three-photon absorption. From previous reports on excited state absorption, it is clear that under the right conditions two successive one-photon absorption processes, with the second an excited state absorption, mimics two-photon absorption.[57] Therefore another option is three-photon absorption into the $1B_u$ state, followed by a one-photon excited state absorption to the mA_g state. This can be labeled as $(3+1)$. Both processes are also resonantly enhanced.

All the parameters are known in order to estimate the impact of the $(3+1)$ process. It is known that the excited state transition dipole moment μ_{12} is one to two times μ_{01}, the one-photon electric dipole transition element from the ground state to $1B_u$.[4,48] The saturation intensity for the $1A_g$ to $1B_u$ transition has been measured to be 65 MW/cm^2.[15] Taking into account the factor of 20 difference in the upper state lifetimes between the one-photon absorption from the $1A_g$ and $1B_u$ states versus the $1B_u$ to the mA_g states, we estimate the saturation intensity for the excited state absorption to be of the order of 1–2 GW/cm^2. Thus for the intensities used in the current experiments, 10's GW/cm^2, most electrons excited to the $1B_u$ state by three-photon absorption which occurs primarily at the peak of the pulses undergo an immediate 1 photon excited state absorption to mA_g.

A very simple model is assumed to explain the impact of this saturation on the $3+1$ process of excited state absorption. For simplicity it is assumed that both the $1B_u$ and mA_g levels have an ''infinite'' lifetime, so that if the electron gets excited to either one, it does not have a chance to decay and be reabsorbed. The relevant rate equations for the $3+1$ process are

$$\Delta N_{1Ag} = -\frac{N_{1Ag}}{N_0}\frac{\alpha_3}{3\hbar\omega} I^3 d^3 V dt,$$

$$\Delta N_{1Bu} = \left[\frac{N_{1Ag}}{N_0}\frac{\alpha_3}{3\hbar\omega} I^3 - \frac{N_{1Bu}}{N_0}\frac{\alpha_{\mathrm{ES}}}{\hbar\omega} I\right] d^3 V dt,$$

$$\Delta N_{mAg} = \frac{N_{1Bu}}{N_0}\frac{\alpha_{\mathrm{ES}}}{\hbar\omega} I d^3 V dt,$$

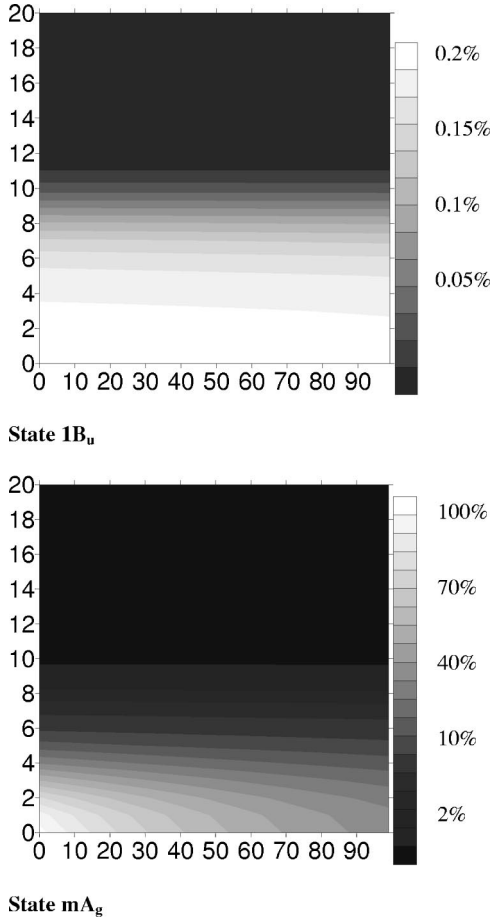

FIG. 14. The contour plot of excited electron population density immediately after propagation of a 100 fs Gaussian pulse with the peak intensity of ~30 GW/cm^2 (%, normalized to the maximal electron population density of mA_g state) in the $1B_u$ and mA_g states as a function of distance into the crystal (x axis, μm) and radial beam coordinate (y axis, μm). Note the factor of 500 between the gray scales for the two states.

where the intensity and all the populations N depend on the spatial and temporal coordinates, i.e., x, y, z, t, and d^3V is a small volume element. A Gaussian input beam is assumed and therefore the complex beam dynamics in both space and time is included. The initial conditions correspond to a non-excited medium, i.e., $N_{1Ag}=N_0$; $N_{1Bu}=0$ and $N_{mAg}=0$, where N_0 is the initial electron density; and α_{ES} corresponds to the one-photon excited state absorption coefficient under the assumption that all electrons are in $1B_u$ state.

Numerical solutions of these equations based on PTS parameters at input intensities of 10's GW/cm^2 for beams Gaussian in space and time show that indeed about 95 to 99 % of the electrons excited into the $1B_u$ exciton state get promoted via consecutive one photon absorption to end up in the mA_g level within the duration of a 100 fs pulse. For input intensities less than the estimated saturation intensity for the $1B_u$ to mA_g transition, the $(3+1)$ process indeed leads to absorption proportional to I^3, the same intensity dependence as for four-photon absorption. However, the situation changes when the peak input intensity is much higher than the saturation intensity and the local intensity of the excitation pulse decays towards its tail, more typical of the experimental conditions. Indeed, the ''supply'' of the electrons excited into the $1B_u$ state is reduced with the decreasing intensity as I^2, and the probability of one-photon excited state absorption does not change at all. The populations in both states are shown in Fig. 14 after the passage of the pulse. In this limiting case of high intensities for which all the excited state electrons are promoted to mA_g, the overall absorption, shown in Fig. 15, has the same dependence on pulse peak intensity as three-photon absorption itself, i.e., it is proportional to I^2 but with a coefficient larger than the true α_3. In this simple model, the additional contribution of excited state absorption, however, is limited to $\frac{1}{3}$ of the energy absorbed via 3PA. That is the effective three-photon absorption coefficient is $1.33\alpha_3$. This situation is complicated by the lifetime of the mA_g state back to the $1B_u$ state of about 100 fs, i.e., of the order of the pulse widths used.[46] However, since the population of the $1B_u$ state is replenished by decay from the mA_g state, this is expected to simply enhance the effective three-photon coefficient further. On the other hand the 4PA process$\propto I^3$ has a different dependence on input peak intensity, as it has a faster rate of growth with intensity, which overtakes 3PA (and therefore the 3PA+excited state) contribution for peak intensities of 30 GW/cm^2 and higher. We therefore conclude that the absorption process we observe in the experiment proportional to I^3 is instantaneous four-photon absorption, enhanced by the near degeneracy with the three-photon absorption.

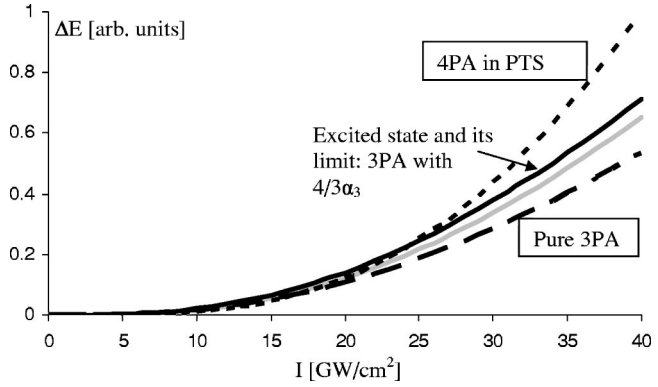

FIG. 15. Three-, four-, and excited-state absorption in PTS probed by 100 fs pulsed beam. Energy absorbed by different processes, regular three-photon absorption (black dashed), regular three-photon absorption with $1.33\alpha_3$, illustrative purposes (black solid), $3+1$ saturated excited state absorption (gray solid), and four-photon regular absorption (black dotted).

VII. SUMMARY

The nonlinear optical response of a prototypical single crystal polydiacetylene (PTS) has been measured in the wavelength range 1200 to 2200 nm. In this region, both the nonlinear refraction and two-photon absorption coefficients decayed monotonically with increasing wavelength. This was expected because of the large two-photon resonance previously observed at 930 nm. Both of these processes exhibited the long wavelength tail of this resonance.

The three- and four-photon absorption response exhibited maxima at wavelengths predicted from the previously measured one- and two-photon absorption spectra. The three-photon absorption measured was weak, as expected, but there were features in the dispersion with wavelength that are not completely understood. The two step process of three-photon absorption followed by a one-photon absorption process was analyzed and found to contribute to the population of the final state, but not to contribute to the measured four-photon absorption coefficient at the intensities used. The measured four-photon absorption coefficient is the instantaneous three-photon enhanced four-photon coefficient. It was observable only because of the exact degeneracy with three-photon enhancement.

ACKNOWLEDGMENT

This research was supported by NSF Grant No. ECS-98-70759.

*Current address: California Institute of Technology, Department of Physics, Mathematics and Astronomy, MC 12-33 Pasadena, CA 91125.

†Current address: University of Toronto, Dept. of Electrical & Computer Engineering, 10 King's College Road, Toronto, Ontario M5S 3G4, Canada.

‡Current address: Chorum Technology, 1303 E. Arapaho Road, Richardson, TX 75081.

[1] Reviewed in G. Wegner, in *Molecular Metals*, edited by W. E. Hatfield (Plenum Press, New York, 1979), p. 209.

[2] Reviewed in *Polydiacetylenes*, Vol. 102 of *NATO Advanced Studies Institute, Series E: Applied Sciences*, edited by D. R. Bloor and R. R. Chance (Martinus Najhoff, The Netherlands, 1985).

[3] Articles in *Polydiacetylenes, Advances in Polymer Science*, edited by H. J. Cantow (Springer-Verlag, Berlin, 1984), No. 63.

[4] D. Mukhopadhyay and Z. G. Soos, J. Chem. Phys. **104**, 1600 (1996).

[5] Discussed in L. Salem, *The Molecular Orbital Theory of Conjugated Systems* (Benjamin, New York, 1966); H. Suzuki, *Electronic Absorpton Spectra and Geometry of Organic Molecules* (Academic Press, New York, 1967).

[6] For example, G. J. Blanchard, J. P. Heritage, G. L. Baker, and S. Etemad, Chem. Phys. Lett. **158**, 329 (1989).

[7] For example, R. H. Austin, G. L. Baker, S. Etemad, and R. Thompson, J. Chem. Phys. **90**, 6642 (1989).

[8] For example, A. S. Siddiqui, J. Phys. C **13**, 2147 (1980).

[9] C. Sauteret, J. P. Hermann, R. Frey, F. Pradere, J. Ducuing, R. H. Baughman, and R. R. Chance, Phys. Rev. Lett. **36**, 956 (1976).

[10] M. Lequime and J. P. Hermann, Chem. Phys. **26**, 431 (1977).

[11] F. Kajzar and J. Messier, Polym. J. (Tokyo, Jpn.) **19**, 275 (1987); **19**, 275 (1987); in *Nonlinear Optical Properties of Organic Molecules and Crystals*, edited by D. Chemla and J. Zyss (Academic Press, New York, 1987), Vol. 2, Chap. 3.

[12] J. M. Nunzi and F. Charra, Nonlinear Opt. **1**, 19 (1991).

[13] F. Charra, J. M. Nunzi, in *Organic Molecules for Nonlinear Optics and Photonics*, edited by J. Messier (Kluwer Academic Publishers, The Netherlands, 1991), pp. 359–368.

[14] G. M. Carter, Y. J. Chen, and S. K. Tripathy, Opt. Eng. **24**, 609 (1984).

[15] J. Bolger, T. G. Harvey, W. Ji, A. K. Kar, S. Molyneux, B. S. Wherrett, D. Bloor, and P. Norman, J. Opt. Soc. Am. B **9**, 1552 (1992).

[16] P. A. Gass, I. Abram, R. Raj, and M. Schott, J. Chem. Phys. **100**, 88 (1994).

[17] D. Y. Kim, B. L. Lawrence, W. E. Torruellas, G. I. Stegeman, G. Baker, and J. Meth, Appl. Phys. Lett. **65**, 1742 (1994).

[18] A. K. Bhowmik and M. Thakur, Opt. Lett. **26**, 902 (2001).

[19] M. C. Gabriel, N. A. Whitaker, C. W. Dirk, M. G. Kuzyk, and M. Thakur, Opt. Lett. **16**, 1334 (1991).

[20] D. M. Krol and M. Thakur, Appl. Phys. Lett. **56**, 1406 (1990).

[21] B. L. Lawrence, M. Cha, W. E. Torruellas, G. I. Stegeman, S. Etemad, and G. Baker, Appl. Phys. Lett. **64**, 2773 (1994).

[22] B. L. Lawrence, M. Cha, W. E. Torruellas, G. I. Stegeman, S. Etemad, and G. Baker, J. Nonlinear Opt. Phys. Mater. **9**, 193 (1995).

[23] B. Lawrence, W. Torruellas, M. Cha, G. I. Stegeman, J. Meth, S. Etemad, and G. Baker, Phys. Rev. Lett. **73**, 597 (1994).

[24] W. E. Torruellas, B. L. Lawrence, G. I. Stegeman, and G. Baker, Opt. Lett. **21**, 1777 (1996).

[25] For example, M. L. Shand and R. R. Chance, J. Chem. Phys. **69**, 4482 (1978).

[26] R. R. Chance, M. L. Shand, C. Hogg, and R. Silbey, Phys. Rev. B **22**, 3540 (1980).

[27] D. Bloor, L. Koski, G. C. Stevens, F. H. Preston, and D. J. Ando, J. Mater. Sci. **10**, 1678 (1975).

[28] G. I. Stegeman and A. Miller, in *Photonic Switching*, edited by J. Midwinter (Academic Press, Orlando, 1992), Vol. 1, pp. 81–146.

[29] K. Sasaki, K. Fujii, T. Tomioka, and T. Kinoshita, J. Opt. Soc. Am. **5**, 457 (1988).

[30] K. Sasaki, S. Sasaki, and O. Furukawa, in *Electrical, Optical and Magnetic Properties of Organic Solid State Materials*, Mater. Res. Soc. Symp. Proc. No. 247, edited by L. Y. Chiang, A. F. Garito, and D. J. Sandman (Materials Research Society, Warrendale, 1992), pp. 141–9.

[31] P. D. Townsend, J. L. Jackel, G. L. Baker, J. A. Shelbourne III, and S. Etemad, Appl. Phys. Lett. **55**, 1829 (1989).

[32] R. Quintero-Torres and M. Thakur, Appl. Phys. Lett. **66**, 1310 (1995).

[33] For example, G. S. He, P. P. Markowicz, T-C. Lin, and P. N. Prasad, Nature (London) **415**, 767 (2002).

[34] M. P. Hasselbeck, E. W. VanStryland, and M. Sheik-Bahae, J. Opt. Soc. Am. B **14**, 1616 (1997), and references cited therein.

[35] H. Shim, M. Liu, C. Hwangbo, and G. I. Stegeman, Opt. Lett. **23**, 430 (1998).

[36] M. Liu, S. Polyakov, F. Yoshino, L. Friedrich, and G. I. Stegeman, Proc. SPIE **CR77**, 135 (2000).

[37] Z. G. Soos and S. Ramasesha, Phys. Rev. B **29**, 5410 (1984).

[38] P. C. M. McWilliams, G. W. Hayden, and Z. G. Soos, Phys. Rev. B **43**, 9777 (1991).

[39] S. N. Dixit, D. Guo, and S. Mazumdar, Phys. Rev. B **43**, 6781 (1991).

[40] S. Mazumdar, D. Guo, and S. N. Dixit, J. Chem. Phys. **96**, 6862 (1992).

[41] G. M. Carter, J. V. Hryniewicz, M. Thakur, Y. J. Chen, and S. E. Meyler, Appl. Phys. Lett. **49**, 998 (1986).
[42] B. I. Greene, J. Orenstein, R. R. Millard, and L. R. Williams, Chem. Phys. Lett. **139**, 381 (1987).
[43] J. M. Huxley, P. Mataloni, R. W. Schoenlein, J. G. Fujimoto, E. P. Ippen, and G. M. Carter, Appl. Phys. Lett. **56**, 1600 (1990).
[44] Reviewed in T. Kobayashi, Synth. Met. **49-50**, 565 (1992); Nonlinear Opt. **1**, 101 (1992).
[45] G. I. Stegeman, M. Liu, S. Polyakov, F. Yoshino, and L. Friedrich, Nonlinear Opt. **24**, 1–17 (2000).
[46] Z. G. Soos, D. Mukhopadhyay, and M. Hennessy, Chem. Phys. **210**, 249 (1997).
[47] G. Wegner, Makromol. Chem. **145**, 85 (1971).
[48] M. Dudley and J. N. Sherwood, Mol. Cryst. Liq. Cryst. **93**, 223 (1983).
[49] For example, G. J. Blanchard, J. P. Heritage, G. L. Baker, and S. Etemad, Chem. Phys. Lett. **158**, 329 (1989).
[50] D. Bloor, L. Koski, G. C. Stevens, F. H. Preston, and D. J. Ando, J. Mater. Sci. **10**, 1678 (1975).
[51] M. Sheik-Bahae, A. A. Said, T. H. Wei, D. J. Hagan, and E. W. Van Stryland, IEEE J. Quantum Electron. **26**, 760 (1990).
[52] S. Polyakov, F. Yoshino, and G. I. Stegeman, J. Opt. Soc. Am. B **18**, 1891 (2001).
[53] B. I. Green, J. F. Muller, J. Orenstein, D. H. Rapkine, S. Schmitt-Rink, and M. Thakur, Phys. Rev. Lett. **61**, 325 (1988).
[54] S. Molyneux, A. K. Kar, B. S. Wherrett, T. L. Axon, and D. Bloor, Opt. Lett. **18**, 2093 (1993).
[55] G. Weiser, Phys. Rev. B **45**, 14 076 (1992).
[56] T. Kobayashi, Optoelectron., Devices Technol. **8**, 309 (1993).
[57] A. A. Said, C. Wamsley, D. J. Hagan, E. W. Van Stryland, B. A. Reinhardt, P. Roderer, and A. G. Dillard, Chem. Phys. Lett. **228**, 646 (1994); T. Xia, D. J. Hagan, A. Dogariu, A. A. Said, and E. W. Van Stryland, Appl. Opt. **36**, 4110 (1997).